INTERNATIONAL ATOMIC ENERGY AGENCY
UNITED NATIONS EDUCATIONAL, SCIENTIFIC AND CULTURAL ORGANIZATION

INTERNATIONAL CENTRE FOR THEORETICAL PHYSICS
34100 TRIESTE (ITALY) - P.O.B. 586 - MIRAMARE - STRADA COSTIERA 11 - TELEPHONE: 2240-1
CABLE: CENTRATOM - TELEX 460892-1

H4.SMR/381-15

COLLEGE ON ATOMIC AND MOLECULAR PHYSICS: PHOTON ASSISTED COLLISIONS IN ATOMS AND MOLECULES

(30 January - 24 February 1989)

ELECTRON-ATOM COLLISIONS IN LASER FIELDS

Lecture 1: Relevant collison theory

Lecture 2: Collision theory in presence of radiation fields: laser-atom interactions

Lecture 3: Summary of experimental state of the art

B. BEDERSON

New York University
Graduate School of Arts & Science
New York
U.S.A.

Lecture 1 : general collision theory; electron-atom collision theory.

the seminal papers on "modern" electron-atom collisions with exchange, polarization, angular momentum taken into account are:

I.C. Percival and M.J. Seaton, Phil. Trans. Roy. Soc. London A251, 113 (1958)

and, particularly, "The Theory of Excitation and Ionization by Electron Impact", M.J. Seaton in Atomic and Molecular Processes, Ed. D.R. Bates Academic Press NY 1966 pp 374-420

The earliest (and still excellent) actual such calculations were by E.M. Karule "Effective Cross Sections for Collisions of Electrons with Atoms" Atomic Collisions III, V. Ia. Veldre, Editor, Latvian Academy of Sciences, Institute of Physics, Riga 1965 [English translation: JILA Information Center Report No. 3, U. of Colorado, Boulder 1966] [elastic] and by E.M. Karule and R.K. Peterkop, ibid [elastic + inelastic, above threshold].

The focus of these papers is to apply "standard" time-independent collision theory to electron-atom systems, where all essential, non-relativistic physics is taken into account in a systematic fashion. This leads naturally to laser scattering, since the laser is a prime tool for both preparation and analysis

of the atomic partner in the collision [also used in the generation of polarized electrons]

"Cross section" concept comes from classical collision theory - refers to an effective area associated with some specific binary interaction: the parameter that transforms an incoming particle flux into an outgoing current at some solid angle (θ, ϕ) per unit solid angle per unit incident flux, for a specific reaction

$$j_{out} = \sigma \, I_{in}(\theta, \phi)$$

the literal classical interpretation is an area: if b is the "impact parameter" then $b\,db\,d\Phi = \sigma(\theta, \phi)$

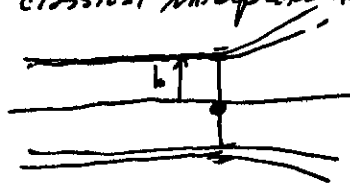

quantum mechanically this gets translated into asymptotic incoming and outgoing wave functions:

$$\Psi^{-}(a, \vec{k}_i; \vec{r}_1, \vec{r}_2) \underset{r_2 \to \infty}{\sim} \psi(\bar{a}, \vec{r}_1) e^{i \vec{k}_i \cdot \vec{r}_2} + \sum_{\text{final states}} \psi(a', \vec{r}_1) f(a', \vec{k}_f; a, \vec{k}_i) \frac{e^{i \vec{k}_f \cdot \vec{r}_2}}{r_2} \quad (1)$$

where a, a' : initial & final atomic states
$\vec{k}_i, \vec{k}_f$: initial & final scattered electron momenta
Ψ^{-} : complete wave function
$\psi(\bar{a}, \vec{r}_1)$, $\psi(a', \vec{r}_1)$: initial & final atomic states

f is the quantity which contains all information concerning the interaction, i.e., the dynamics, the kinematics, the reaction options open to the collision. This is the starting point, generally, of all collision theory. NOTE: f is, in fact, part of the interaction wavefunction. Wavefunctions are not observables in experiment. The theorist must always find a way to convert f into an observable, loosing as little information as possible in making this transition.

The MOST INFORMATION LOST would be when experiment measures all interactions to all final states at all scattering angles and all energies! This would correspond to a beam-gas experiment done in transmission, i.e., an attenuation measurement

$$I = I_0 e^{-\alpha z}$$

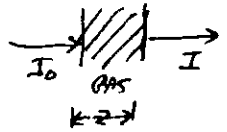

the LEAST information lost corresponds to an experiment in which target + projectile [atom + electron in the present instance] are completely state selected and analyzed, i.e., by energy, momentum, polarization, etc. etc. Modern collision experiments, with and without lasers, has as a general goal the performance of such experiments.

equating input flux to outward current, just as for classical scattering,

$$k_a I(a k_a \to a' k_{a'}) = k_{a'} |f|^2$$

where $|f|^2$, with units of L^2, is the cross section, σ. Therefore the relation of theory to experiment is as f is to $|f|^2$

other considerations:

"exchange" scattering: same as (1), except $r_2 \to r_1$, $r_1 \to r_2$ in scattered wave and there is no incoming plane wave

$$\psi \underset{r_1 \to \infty}{\sim} \sum \psi(a', \vec{r}_2)\, g(a', \hat{k}_f; a, \hat{k}_i) \frac{e^{i k_i \cdot \vec{r}_1}}{r_1} \qquad (2)$$

where now f, g are the direct + exchange scattering amplitudes. In the 2-electron collision problem, [atomic K, alkalis], the direct and exchange amplitudes are related to the singlet + triplet amplitudes f^+, f^-:

$$\left.\begin{aligned} f &= \tfrac{1}{2}(f^+ + f^-) \\ g &= \tfrac{1}{2}(f^+ - f^-) \end{aligned}\right\} \qquad (3)$$

see enclosed notes [Seaton 1966] for complete discussion of all this. To obtain solutions for f's, g's one way is to expand Ψ in terms of the (presumably) known stationary unperturbed atomic wavefunctions:

$$\Psi^{\pm}(\vec{r}_1, \vec{r}_2) = \sum_a \psi(a, \vec{r}_1)\, F^{\pm}(a, \vec{r}_2)$$

etc. which reduce the problem somewhat:

$$\int \psi^*(a, \vec{r}_1)[H - E]\Psi(\vec{r}_1, \vec{r}_2)\, d\vec{r}_1 = 0$$

becomes $$[\nabla^2 + k_a^2] F(a, \vec{r}) = 2 \sum_{a'} V_{aa'}(\vec{r}) F(a', \vec{r})$$

with

$$V_{aa'}(\vec{r}_2) = \int \psi(a, \vec{r}_1) \left[-\frac{1}{r_2} + \frac{1}{r_{12}} \right] \psi(a', \vec{r}_1) \, d\vec{r}_1$$

or, with properly symmetrized wave function,

$$F \to F^{\pm}, \quad V \to V \pm W$$

where $$W_{aa'} = \int \psi^*(a, \vec{r}_1) [H(\vec{r}_1, \vec{r}_2) - E] F(a', \vec{r}_1) d\vec{r}_1 \times \psi(a', \vec{r}_2)$$

$W_{aa'}$ is the exchange operator

Born approximation: ψ scattered $\to$ unperturbed ψ

$$f_{B_1}(a', a) = -\frac{1}{2\pi} \int e^{-i\vec{k}_{a'} \cdot \vec{r}} V_{a'a} e^{i\vec{k}_a \cdot \vec{r}} \, d\vec{r}$$

Born-Oppenheimer approx (properly symmetrized)

$$f_{BO}^{\pm} = -\frac{1}{2\pi} \int e^{-i\vec{k}_{a'} \cdot \vec{r}} [V_{a'a} \pm W_{a'a}] e^{i\vec{k}_a \cdot \vec{r}} \, d\vec{r}$$

"

<u>Percival-Seaton hypothesis</u>: spin-orbit, spin-spin interactions play no role in collision. Pretty good assumption for light atoms, not at resonances. [spin, however, plays an important role in determining allowed solutions to the Schroedinger equation!]

about Oz. The scattered electron cannot have any angular momentum when its velocity tends to zero, and in this limit only $M' = 0$ can be excited. Hence, at threshold, $(Q_1/Q_0) = 0$ and $P = 1$.

The polarization is reduced when fine structure is included and is further reduced by hyperfine structure when the natural linewidth is small compared with the hfs separations. Percival and Seaton consider the case of the Ly-α line of hydrogen for which the width is comparable with the hfs separations.

Skinner and Appleyard (1927) have measured P for a number of Hg lines. At energies not close to thresholds, the general pattern of their results is in agreement with what theory would lead one to expect, but as the excitation thresholds are approached the measurements appear to give P tending to zero. This is illustrated in Fig. 7. There is no satisfactory explanation of this near-threshold behavior of the experimental results.

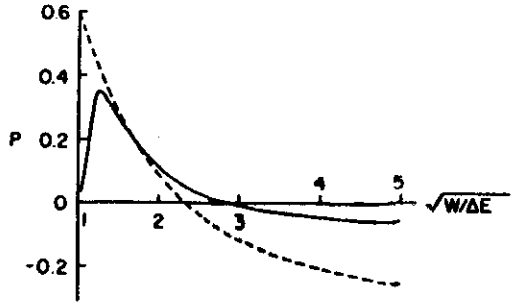

FIG. 7. The polarization fraction for radiative $^1D \rightarrow {}^1P$ transitions without hyperfine structure; P against $\sqrt{W/\Delta E}$. Dashed curve calculated for He $3^1D \rightarrow {}^1P$ (Percival and Seaton, 1958), full line curve, experimental for Hg $7^1D \rightarrow 6^1P$ (Skinner and Appleyard, 1927).

3 *Partial Wave Theory*

The partial wave theory, in which one considers states of definite angular momentum for the colliding electron, is needed for all practical calculations other than those using the Born approximation. In place of the partial differential equations of § 2.5 one obtains differential equations in one variable which may be solved by numerical methods.

The partial wave theory also enables us to obtain much more precise estimates of the reliability of different approximations.

3.1 The Scattering Matrix

The functions

$$\varphi_\pm(klm|r) = k^{-1/2}\, Y_{lm}(\hat{r})\, \frac{\exp \pm i(kr - \frac{1}{2}l\pi)}{r} \tag{83}$$

represent waves with angular momentum lm and a total current of one particle per unit time. The function φ_- represents an incoming wave and φ_+ represents an outgoing wave.

We use quantum numbers $a = nl_1m_1$ for the atomic electron and $k_al_2m_2$ for the colliding electron, and we consider complete wave functions $\Psi_S(al_2m_2|r_1, r_2)$ having asymptotic form

$$\Psi_S(al_2m_2|r_1, r_2) \underset{r_2\to\infty}{\sim} \psi(a|r_1)\, \varphi_-(k_al_2m_2|r_2) - \sum_{a'l_2'm_2'} \psi(a'|r_1)\, \varphi_+(k_{a'}l_2'm_2'|r_2)\, S(a'l_2'm_2', al_2m_2) \tag{84}$$

where **S** is the scattering matrix. For elastic scattering $S(l) = e^{2i\eta_l}$. The condition for conservation of current is†

$$\sum_{\alpha'} |\, S(\alpha, \alpha')\, |^2 = 1. \tag{85}$$

When the coupling is weak for $\alpha \rightarrow \alpha'$ one must have

$$|\, S(\alpha, \alpha')\, | \ll 1.$$

To obtain the scattering amplitude in terms of **S** we require the relations:

$$\exp i\mathbf{k}\cdot\mathbf{r} = \sum_l (2l+1)\, P_l(\hat{\mathbf{k}}\cdot\hat{\mathbf{r}})\, i^l\, \frac{1}{kr} j_l(kr), \tag{86}$$

$$j_l(x) = \left(\frac{\pi x}{2}\right)^{1/2} J_{l+1/2}(x) \underset{x\to\infty}{\sim} \sin(x - \tfrac{1}{2}l\pi), \tag{87}$$

and

$$P_l(\hat{\mathbf{k}}\cdot\hat{\mathbf{r}}) = \left(\frac{4\pi}{2l+1}\right) \sum_m Y_{lm}^*(\hat{\mathbf{k}})\, Y_{lm}(\hat{\mathbf{r}}). \tag{88}$$

† When unsymmetrized functions are used, in (85) we must include contributions from exchange amplitudes.

One obtains

$$f(\alpha' \mathbf{k}_{n'}, \alpha \mathbf{k}_n) = \frac{2\pi i}{(k_n k_{n'})^{1/2}} \sum_{l_2 m_2 l_2' m_2'} Y^*_{l_2' m_2'}(\hat{\mathbf{k}}_n)\, Y_{l_2 m_2}(\hat{\mathbf{k}}_{n'})\, i^{l_2 - l_2'}\, T(\alpha' l_2' m_2', \alpha l_2 m_2) \tag{89}$$

where

$$T(\alpha', \alpha) \equiv \delta(\alpha', \alpha) - S(\alpha', \alpha) \tag{90}$$

defines an element of the transmission matrix, T. On substituting in (19) we obtain†

$$Q(nl_1 \to n'l_1') = \frac{\pi}{k_n^2} \cdot \frac{1}{(2l_1 + 1)} \sum_{m_1 m_1'} \sum_{l_2 l_2'} \sum_{m_2 m_2'} |\, T(n'l_1'm_1'l_2'm_2', nl_1m_1l_2m_2) \,|^2. \tag{91}$$

A simpler expression is obtained on introducing the total angular momentum, LM. Define

$$\Phi_\pm(nl_1l_2LM|\mathbf{r}_1, \mathbf{r}_2) = \sum_{m_1 m_2} C^{l_1 l_2 L}_{m_1 m_2 M}\, \psi(nl_1m_1|\mathbf{r}_1)\, \varphi_\pm(k_n l_2 m_2|\mathbf{r}_2) \tag{92}$$

and let

$$\Psi_S(\alpha|\mathbf{r}_1, \mathbf{r}_2) \underset{r_2 \to \infty}{\sim} \Phi_-(\alpha|\mathbf{r}_1, \mathbf{r}_2) - \sum_{\alpha'} \Phi_+(\alpha'|\mathbf{r}_1, \mathbf{r}_2)\, S(\alpha', \alpha). \tag{93}$$

The matrix $S(n'l_1'l_2'L'M', nl_1l_2LM)$ is diagonal with respect to LM, since the total angular momentum does not change, and is independent of M, this quantum number serving only to define the orientation of the entire system with respect to some arbitrary direction. The S matrix satisfies transformation relations of the type

$$S(l_1'm_1'l_2'm_2', l_1m_1l_2m_2) = \sum_{LM} C^{l_1' l_2' L}_{m_1' m_2' M} S(l_2'l_2'L, l_1l_2L)\, C^{l_1 l_2 L}_{m_1 m_2 M}. \tag{94}$$

Equation (91) becomes

$$Q(nl_1 \to n'l_1') = \frac{\pi}{k_n^2} \frac{1}{(2l_1 + 1)} \sum_{l_2 l_2' L} (2L + 1)\, |\, T(n'l_1'l_2'L, nl_1l_2L) \,|^2. \tag{95}$$

† Expression (19) is independent of the direction of $\mathbf{k}_n$. The simplest derivation of (91) is obtained on integrating (19) over $d\hat{\mathbf{k}}$ and dividing by 4π.

When we include spin variables and use antisymmetric functions $\Psi(\mathbf{x}_1, \mathbf{x}_2)$, we obtain

$$Q(nl_1 \to n'l_1') = \frac{\pi}{k_n^2} \cdot \frac{1}{4(2l_1 + 1)} \sum_{l_2 l_2' SL} (2L + 1)\,(2S + 1)\, |\, T(n'l_1'l_2'SL, nl_1l_2SL) \,|^2. \tag{96}$$

These expressions may be compared with the classical theory (§ 1); $|\, T(\alpha', \alpha) \,|^2$ is the quantity corresponding to $P_{ss'}$.

3.2 The Reactance Matrix

It is usually convenient to work with real functions. We define

$$\varphi_{\binom{s}{c}}(klm|\mathbf{r}) = k^{-1/2}\, Y_{lm}(\hat{\mathbf{r}})\, \frac{1}{r} \begin{pmatrix} \sin \\ \cos \end{pmatrix} (kr - \tfrac{1}{2} l\pi) \tag{97}$$

and Φ_s, Φ_c by relations similar to (92). The R matrix is defined by a function Ψ_R having asymptotic form

$$\Psi_R(\alpha) \sim \Phi_s(\alpha) + \sum_{\alpha'} \Phi_c(\alpha')\, R(\alpha', \alpha). \tag{98}$$

On using

$$2i\Phi_s = \Phi_+ - \Phi_-, \qquad 2\Phi_c = \Phi_+ + \Phi_- \tag{99}$$

one obtains

$$\mathbf{S} = \frac{1 + i\mathbf{R}}{1 - i\mathbf{R}}. \tag{100}$$

For elastic scattering, $R(l) = \tan \eta_l$.

3.3 Properties of the R and S Matrices

In the representation

$$\alpha = nl_1l_2SL \tag{101}$$

and with the usual phase conventions (Edmonds, 1957) it may be shown that R is real and symmetric,

$$\mathbf{R} = \mathbf{R}^* = \tilde{\mathbf{R}}, \tag{102}$$

and that S is unitary and symmetric,

$$\mathbf{S}^\dagger\mathbf{S} = \mathbf{1}, \qquad \mathbf{S} = \tilde{\mathbf{S}} \tag{103}$$

The conservation relation (85) is a special case of the unitary property. From $S = \tilde{S}$ we obtain the reciprocity relations, such as

$$(2l_1 + 1)\, k_n^2\, Q(nl_1 \to n'l_1') = (2l_1' + 1)\, k_{n'}^2\, Q(n'l_1' \to nl_1). \tag{104}$$

3.4 Radial Equations

Let us define

$$\Phi(nl_1l_2L|\mathbf{r}_1, \mathbf{r}_2) = \sum_{m_1m_2} C^{l_1l_2L}_{m_1m_2M}\, \psi(nl_1m_1|\mathbf{r}_1)\, Y_{l_2m_2}(\hat{\mathbf{r}}_2)\, \frac{1}{r_2}\, F(nl_1l_2L|r_2) \tag{105}$$

and let the complete wave function be

$$\Psi^\pm(\alpha) = \frac{1}{\sqrt{2}} \sum_{\alpha'} \{\Phi(\alpha'|\mathbf{r}_1, \mathbf{r}_2) \pm \Phi(\alpha'|\mathbf{r}_2, \mathbf{r}_1)\}. \tag{106}$$

For the radial functions $F(\alpha)$ one obtains equations of the form

$$\left\{\frac{d^2}{dr^2} - \frac{l_2(l_2+1)}{r^2} + k^2\right\} F(\alpha) = 2 \sum_{\alpha'} \{V_{\alpha\alpha'} \pm W_{\alpha\alpha'}\}\, F(\alpha'). \tag{107}$$

These are discussed in detail by Percival and Seaton (1957).

3.5 Variational Principles

For any symmetrized function $\Psi_f\ (= \Psi_f^\pm)$ with asymptotic form

$$\Psi_f(\alpha) \underset{r_2\to\infty}{\sim} \frac{1}{\sqrt{2}} \left\{\Phi_s(\alpha|\mathbf{r}_1, \mathbf{r}_2) + \sum_{\alpha'} \Phi_c(\alpha'|\mathbf{r}_1, \mathbf{r}_2)\, R_f(\alpha', \alpha)\right\}, \tag{108}$$

define

$$L_f(\alpha, \alpha') = \int \Psi_f^*(\alpha)\, [H - E]\, \Psi_f(\alpha')\, d^3\mathbf{r}_1\, d^3\mathbf{r}_2. \tag{109}$$

By a generalization of the argument giving the Hulthén and Kohn variational principles for elastic scattering (Chapter 9, § 1.7) it may be shown that

$$R(\alpha, \alpha') = R_f(\alpha, \alpha') - 2L_f(\alpha, \alpha') + 2 \int \delta\Psi^*(\alpha)\, [H - E]\, \delta\Psi(\alpha')\, d^3\mathbf{r}_1\, d^3\mathbf{r}_2 \tag{110}$$

where $\delta\Psi = \Psi_f - \Psi$, Ψ being the exact wave function and R the exact reactance matrix. Given any approximate wave function Ψ_f, with corresponding R_f, an improved estimate for R is

$$\mathbf{R}_K = \mathbf{R}_f - 2\mathbf{L}_f. \tag{111}$$

3.6 Weak Coupling Approximations

In weak coupling approximations one first obtains functions

$$\Psi_f(\alpha) = \frac{1}{\sqrt{2}} \{\Phi_f(\alpha|\mathbf{r}_1, \mathbf{r}_2) \pm \Phi_f(\alpha|\mathbf{r}_2, \mathbf{r}_1)\} \tag{112}$$

neglecting the coupling, so that $R_f(\alpha, \alpha') = 0$ for $\alpha \neq \alpha'$, and then calculates

$$R_K(\alpha, \alpha') = -2L_f(\alpha, \alpha'). \tag{113}$$

In terms of the radial functions this gives

$$R_K(\alpha, \alpha') = -2 \int F(\alpha|r)\, [V_{\alpha\alpha'} \pm W_{\alpha\alpha'}]\, F(\alpha'|r)\, dr. \tag{114}$$

In the exchange distorted wave method one would have

$$\left\{\frac{d^2}{dr^2} - \frac{l_2(l_2+1)}{r^2} - 2(V_{\alpha\alpha} \pm W_{\alpha\alpha}) + k_\alpha^2\right\} F(\alpha|r) = 0, \tag{115}$$

$$F(\alpha|r) \sim k_\alpha^{-1/2} \{\sin(k_\alpha r - \tfrac{1}{2} l_2\pi) + \cos(k_\alpha r - \tfrac{1}{2} l_2\pi)\, R_f(\alpha, \alpha)\}. \tag{116}$$

In the Born approximation one uses†

$$F_B(\alpha|r) = k_\alpha^{-1/2} j_{l_2}(k_\alpha r) \tag{117}$$

and neglects $W_{\alpha\alpha'}$ in (114).

† j_l is defined by (87).

Eq. 89 of the Seaton article can be simplified by taking advantage of angular momentum conservation laws. Instead of using $l_2 m_2$, $l_2' m_2'$, a, a', why not use $L M_L$, the total momentum of atom + free electron? Since these are conserved in the collision, resulting scattering amplitude will be greatly simplified.

start with:

$$f(a'\hat{R}_{a'}, a\hat{k}_a) = \frac{2\pi i}{(k_a k_{a'})^{1/2}} \sum_{\substack{l_2 m_2 \\ l_2' m_2'}} Y^*_{l_2 m_2}(\hat{k}_a)\, Y_{l_2' m_2'}(\hat{R}_{a'})\, i^{l_2 - l_2'} \times$$

$$\times\, T^{\pm}(a' l_2' m_2', a l_2 m_2)$$

summary of definitions:

T is the "transmission matrix", related to the "scattering matrix" S by

$$T(\alpha', \alpha) = \delta(\alpha', \alpha) - S(\alpha', \alpha)$$

T can be defined in terms of a real matrix R, defined by

$$T = -2iR(1 - iR)^{-1}$$

unprimes = initial state — $l_2\, m_2$: orbital angular momentum of incoming electron

primes = final state — $l_2'\, m_2'$: " " " "outgoing"

a, a': atomic quantum numbers of initial + final states

$\hat{k}_a$ ($\hat{R}_{a'}$): unit vector in direction of incident (scattered) electron

k_a ($k_{a'}$): initial (final) wave number, i.e., momentum $= \frac{\hbar}{i}\left(\frac{\partial}{\partial x}\right)$

L, M_L: total ang. mom and projection along axis of quantization

the superscripts in $f^{\pm}$, $T^{\pm}$ refer to the 2-electron (1,2) system i.e., atomic H or alkali. The + is singlet [antisymmetric spin function, symmetric space function], the − is triplet [symmetric spin wave function, antisymmetric space function]

Reduction of the Summation: Proper choice of quantization axis.

Choose the direction $\hat{k}$ as the direction of the quantization axis z

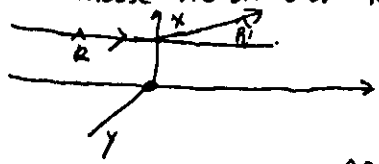

define the scattering plane so that $\frac{\hat{k} \times \hat{R}'}{|\hat{k} \times \hat{R}'|}$ is a unit vector in y-direction

so x-z is the scattering plane.

thus $\vec{l}_2$ is along y and so $m_2 = 0$

and $Y^*_{l_2 m_2}(\omega\Theta) = Y^*_{l_2, 0}(1) = \sqrt{\frac{2l_2+1}{4\pi}}$ [because $\int \psi^* \psi\, d\Omega = 1$]

so $\sum_{\substack{l_2 m_2 \\ l_2' m_2'}} \to \sum_{\substack{l_2 \\ l_2' m_2'}} \sqrt{\frac{2l_2+1}{4\pi}}\, Y_{l_2' m_2'}(\hat{R}_{a'})\, i^{l_2 - l_2'} \ldots$

or, putting in atomic quantum numbers, (leave out $\pm$)

$$f(n,0,0; n\rho\, m_a') = \frac{2\pi i}{(k_a k_{a'})^{1/2}} \frac{1}{\sqrt{4\pi}} \times$$

$$\sum_{\substack{l_2 \\ l_2' m_2'}} Y_{l_2' m_2'}(\hat{k}_{a'})\, i^{l_2 - l_2'}\, T(m_a', l_2', m_2'; m_a = 0, l_2, m_2 = 0) \sqrt{2l_2+1}$$

Conservation rules

(1) $m_a + m_2 = m_{a'} + m_2' = M = 0$, so

$m_{a'} = -m_2'$, eliminating the m_2' summation

(2) $|\vec{l}_a + \vec{l}_2| = L = |\vec{l}_{a'} + \vec{l}_{2'}| = |l_2|$

(assuming $l_a = 0$)

since we assume an $s \to p$ transition, $l_{a'} = 1$

$l_{2'} = l_2 \pm 1$

$$f(n,0,0;\, n,1,m_{a'}) = \frac{2\pi i}{(k_a k_{a'})^{1/2}} \frac{1}{4\pi} \sum_{\substack{l_2 \\ l_{2'}}} Y_{l_{2'}, -m_{a'}}(\hat{k}_a)\, e^{i(l_2 - l_{2'})} \times$$

$$\times\ T(m_{a'}, l_{2'}, -m_{a'};\ 0, l_2, 0)\sqrt{2l_2+1}$$

Now we transform from the uncoupled T representation (given in terms of $(a, l_2, m_2;\ a', l_{2'}, m')$ to the coupled representation. The transformation is

$$T\Big(\underbrace{n s,\ m_a = 0}_{\text{atom}} \mid \underbrace{l_2, m_2 = 0}_{\text{electron}};\ \underbrace{n p,\ m_{a'}}_{\text{atom}} \mid \underbrace{l_{2'}, m_{2'} = -m_{a'}}_{\text{electron}}\Big)$$

Before — after

$$= C^{l\ l_{2'}\ L=l_2}_{m_a,\ m_{2'}=-m_{a'};\ M=0}\ T(n s, l_2, L;\ n p, l_{2'} = L \pm 1,\ L)$$

with $C^{l_1 l_2 L}_{m_1 m_2 -M}$ are the Clebsch-Gordan angular momentum coupling coefficients that form L, M from $l_1 + l_2$, $m_1 + m_2$

for $s \to p$ excitation, define

$T_{12} = T(n s,\ L, L;\ n p\ L+1, L)$

$T_{13} = T(n s, L, L;\ n p\ L-1, L)$

$C_{12} = C^{l, L+1, L}_{m_a', -m_a', 0}$; $C_{13} = C^{l, L-1, L}_{m_a', -m_a', 0}$

to 12 term $i^{l_2 - l_2'} = i^{-1}$; 13 term $i^{l_2 - l_2'} = i^{+1}$

so altogether

$$f^{\pm}(n00;\, npm_a) = \frac{\sqrt{8\pi}}{\sqrt{k_a k_a' R_a R_a'}} \sum_{L=1}^{\infty} \Big[Y_{L+1, -m_a'}(\theta,\varphi)\, C^{l, L+1, L}_{m_a', -m_a', 0}\, T^{L\pm}_{12}$$

$$- Y_{L-1, -m_a'}\, C^{l, L-1, L}_{m_a', -m_a', 0}\, T^{L\pm}_{13} \Big] \sqrt{2L+1} \quad (4)$$

sometimes easier to compute the R-matrix (see page 10) from which it is easy to get T:

$$T = -2iR(1+iR)[(1-iR)(1+iR)]^{-1}$$

$$= -2iR(1+iR)(1+R^2)^{-1} = (-2iR + 2R^2)(1+R^2)^{-1}$$

so $\quad \mathrm{Im}\ Pt\ T = -2R(1+R^2)^{-1}$

$$\mathrm{Re}\ Pt\ T = -R\ \mathrm{Im}\ T$$

note that while T is complex, R is real and symmetric

$$(s \to p)\, T = \begin{pmatrix} T_{11} & T_{12} & T_{13} \\ T_{21} & \cdot & \cdot \\ T_{31} & \cdot & \cdot \end{pmatrix}$$

Elastic, Inelastic, Superelastic scattering (one-electron atoms)

the laser can be used to prepare atomic systems into selected excited states, from which they can be scattered either elastically (though with possible change of M_L, M_S), inelastic — transitions to higher lying levels, or "superelastic" — induced collisions to lower lying levels. the last process is related by detailed balancing to the inverse inelastic process. Accordingly Eqn 4 can be generalized to include T-matrix elements

T_{11} (ground-state elastic scattering) T_{22}, T_{99} (excited-state scattering $L-1 \to L-1$; $L+1 \to L+1$) T_{23}, T_{32} (ditto, $L \to L+1$; $L \to L-1$)

$$T = \begin{pmatrix} T_{11} & T_{12} & T_{13} \\ T_{21} & T_{22} & T_{23} \\ T_{31} & T_{32} & T_{33} \end{pmatrix} \sim \begin{pmatrix} \text{adiabatic} \\ \text{elastic} \\ \text{excited} \\ \text{inelastic} \end{pmatrix}$$

the hard physics is in the solution of the radial equations

to show you how hard this is, I include, the famous computations "2-state" close coupling calculations of Karule & Peterkop (1966) — the full work is published in English translation as JILA Information Center Report No. 3, University of Colorado 1966. Only T_{11}, T_{12}, T_{13} were calculated [they had no idea that it would be possible to measure T_{22}, etc]. This work also shows explicitly how exchange is taken into account.

I have so far ignored the spin-orbit interaction which mixes excited states, since J, M_J rather than L, M_L; S M_S are conserved (generally) in electron-light atom collisions. this is a whole other story. However, using laser prepared excited states it is sometimes possible to reduce back to the L-representation. More later.

Atomic Collisions III Latvian Academy of Sciences

from E.M. Karule, R.K. Peterkop (1966) "Effective cross-sections for collisions of electrons with atoms"

Using experimental values of oscillator strengths, we also recognize that the coupling with the first excited state provides 98-99% of the polarizability of the alkali atom. In this respect the alkali metals differ advantageously from hydrogen, in which the coupling with the 2p state provides only 65.8% of the polarizability [16].

Shown below, for comparison, are the first five components of polarizability (in a_0^3) for H, Li and Cs:

	n_0	n_0+1	n_0+2	n_0+3	n_0+4
H	2,96	0.56	0.13	0.060	0.033
Li	163	0.28	0.17	0.099	0.057
Cs	429	1.6	0.22	0.056	0.027

Theoretical data [17] were utilized for hydrogen, while experimental values of oscillator strengths and energy levels [18,19] were used for lithium and cesium. It is obvious that the higher components of Li and Cs are on the order of those for hydrogen, while the first is much greater.

SYSTEM OF EQUATIONS

If we disregard spin-orbit interaction, we can use the notion of a total orbital momentum L and projection M [20]. In the approximation which takes into consideration exchange and the strong coupling $n_0s - n_0p$, the wave function describing the incident and the valence electrons has the form

$$\Phi_L = \sum_{l_1}^{l} F_{Ll}(r_1) R_{n_0 l}(r_2) Y_{tLM}(\Omega_1 \Omega_2) \pm (r_1 \rightleftarrows r_2), \qquad (5)$$

Final

where l is the momentum of the incident electron; t is the momentum of the atomic electron; Y_{tLM} is the proper function of operators t, l, L and M.

The "+" sign refers to the symmetrical (singlet) case; the "-" sign refers to the antisymmetrical (triplet) case.

The following values of l and t are possible:

l = elastic	1)	$l = l_1 \equiv L$,	$t = 0$;
	2)	$l = l_2 \equiv L+1$,	$t = 1$;
	3)	$l = l_3 \equiv L-1$,	$t = 1$.

(6)

The first case corresponds to elastic scattering, the second corresponds to excitation of the n_0p level with wave scattering with momentum of L + 1, and the third corresponds to excitation of the n_0p level during which an electron with a momentum of L - 1 is scattered. The third case does not occur at L = 0. Thus at L > 0 the sum (5) comprises three terms, but at L = 0 it comprises two terms.

Henceforth the subscript 1 will correspond to the first case, and 2 and 3 to the second and third.

Since we have to carry out solutions of Hartree-Fock type equations [20], we have prepared a system of integro-differential equations, which can be written briefly in the form

$$\left[\frac{d^2}{dr^2} - \frac{l_i(l_i+1)}{r^2} + k_i^2\right] F_i(r) = -2\sum_{j=1}^{3}\left[V_{ij}(r)F_j(r) \pm \int_0^\infty G_{ij}(r,r')F_j(r')dr'\right], \quad i,j=1,2,3 \tag{7}$$

where

$$k_i^2 = 2(E-\varepsilon_i); \quad \varepsilon_1 = \varepsilon_{n_0 0}; \quad \varepsilon_2 = \varepsilon_3 = \varepsilon_{n_0 1}; \tag{8}$$

E is the energy of the two-electron system.

The matrix of the potentials is real and hermitian:

$$V_{ji}(r) = V_{ij}(r); \quad G_{ji}(r,r') = G_{ij}(r',r). \tag{9}$$

The expressions for potentials are analogous to the expressions in the case of scattering on hydrogen [20].

The non-exchange potentials are equal:

$$\begin{aligned}
V_{11}(r) &= V(r) + y_0(1,1;r);\\
V_{12}(r) &= -\sqrt{\frac{L+1}{3(2L+1)}}\, y_1(1,2;r);\\
V_{13}(r) &= \sqrt{\frac{L}{3(2L+1)}}\, y_1(1,3;r);\\
V_{22}(r) &= V(r) + y_0(2,2;r) + \frac{L+2}{5(2L+1)} y_2(2,2;r);\\
V_{23}(r) &= -\frac{3\sqrt{L(L+1)}}{5(2L+1)} y_2(2,3;r);\\
V_{33}(r) &= V(r) + y_0(3,3;r) + \frac{L-1}{5(2L+1)} y_2(3,3;r),
\end{aligned} \tag{10}$$

where

$$y_k(ij;r) = \int_0^\infty u_i(x)\gamma_k(r,x)u_j(x)dx; \tag{11}$$

$$\gamma_k(r,x) \begin{cases} = r^{-k-1}x^k, & r>x; \\ = r^k x^{-k-1}, & r<x; \end{cases} \tag{12}$$

$$u_1(r) = rR_{n_0 0}(r); \quad u_2 = u_3 = rR_{n_0 1}(r). \tag{13}$$

Exchange potentials G_{ij} can be written in the form

$$G_{ij}(r,r') = u_j(r)u_i(r')\Gamma_{ij}(r,r'), \tag{14}$$

where

$$\Gamma_{ij}(r,r') = \Gamma_{ji}(r,r') = \Gamma_{ij}(r',r); \tag{15}$$

$$\begin{aligned}
\Gamma_{11}(r,r') &= C_{11}[\delta_{L0}(2\varepsilon_1 - E) + \gamma_L(r,r')];\\
\Gamma_{12}(r,r') &= C_{12}\gamma_{L-1}(r,r');\\
\Gamma_{13}(r,r') &= C_{12}[\delta_{L1}(\varepsilon_1+\varepsilon_2-E) + \gamma_{L-1}(r,r')];\\
\Gamma_{22}(r,r') &= C_{22}\gamma_{L+2}(r,r') + C_{22}^{(2)}[\delta_{L0}(2\varepsilon_2 - E) + \gamma_L(r,r')];\\
\Gamma_{23}(r,r') &= C_{23}\gamma_L(r,r');\\
\Gamma_{33}(r,r') &= C_{33}[\delta_{L2}(2\varepsilon_2 - E) + \gamma_{L-2}(r,r')] + C_{33}^{(2)}\gamma_L(r,r').
\end{aligned} \tag{16}$$

The matrix of coefficients C_{ij} is symmetrical ($C_{ij} = C_{ji}$):

$$\begin{aligned}
C_{11} &= \frac{1}{2L+1}; \quad C_{22} = \frac{3(L+2)}{(2L+3)(2L+5)};\\
C_{12} &= -\frac{\sqrt{3(L+1)}}{(2L+3)\sqrt{2L+1}}; \quad C_{23} = -\frac{3\sqrt{L(L+1)}}{(2L+1)^2};\\
C_{13} &= \frac{\sqrt{3L}}{(2L-1)\sqrt{2L+1}}; \quad C_{33} = \frac{3(L-1)}{(2L-1)(2L-3)};\\
C_{22}^{(2)} &= \frac{3}{(2L+1)^2(2L+3)}; \quad C_{33}^{(2)} = \frac{3}{(2L-1)(2L+1)^2}.
\end{aligned} \tag{17}$$

The exchange potentials can be further transformed to the form

$$G_{ij}(r,r') \begin{cases} = \sum_n D_{ijn} N_{jn}(r) M_{nj}(r'), & r>r', \\ = \sum_n D_{ijn} M_{jn}(r) N_{nj}(r') & r<r', \end{cases} \tag{18}$$

where

$$M_{ij}(r) = u_i(r) r^{\lambda}; \tag{19}$$
$$N_{ij}(r) = u_i(r)[r^{-\lambda-1} + (\varepsilon_i + \varepsilon_j - E)\delta_{\lambda 0}].$$

The exponent λ depends upon the subscripts ij symmetrically ($\lambda_{ij} = \lambda_{ji}$) and it is determined

$$\lambda_{11} = L; \quad \lambda_{12} = L+1; \quad \lambda_{13} = L-1; \tag{20}$$
$$\lambda_{22} = L+2; \quad \lambda_{23} = L; \quad \lambda_{33} = L-2.$$

Coefficients $D_{ij1} = C_{ij}$; $D_{223} = C_{22}^{(3)}$; $D_{332} = C_{33}^{(2)}$, but the remaining $D_{ijn} = 0$.

We note that at several values of L the system of equations (7) does not quite determine the unknown functions unambiguously with the boundary conditions usually imposed (at finite distances). This is related to the ambiguous symmetrized (antisymmetrized) expansion of the wave function of the system according to atomic functions. Without changing the total function to a partial function, atomic functions can be added [21].

Substituting into (5)

$$F_{nLl} = \sum_{n'l'} \alpha(nll; n'l') r R_{n'l'} \tag{21}$$

and requiring that the corresponding sum (where we also sum over quantum numbers n) identically equal zero, we obtain

$$\alpha(nll; n'l') = \mp \delta_{nl}(-1)^{l+l'-L} \alpha(n'l'l; nl). \tag{22}$$

As is seen, the functions corresponding to cases in which the atomic and the scattering electrons have the same moments are ambiguous.

In the approximation we used, the following admixture of atomic states is possible:

At energies above the excitation threshold of the n_0p level, which are examined in the present work, one must find three linearly independent solu of system (7) with asymptotic

$$F_i^{(l)}(\infty) \sim \frac{1}{\sqrt{k_i}}\left[\delta_{ij}\sin\left(k_i r - \frac{l_i\pi}{2}\right) + K_{ij}\cos\left(k_i r - \frac{l_i\pi}{2}\right)\right]. \tag{27}$$

These solutions determine K_{ij} - the elements of the K-matrix. The effective cross sections are expressed as elements of the T-matrix, which we determine according to [33]:

$$T = -2iK(1 - iK)^{-1}. \tag{28}$$

At zero the solutions of system (7) are determined by boundary conditio

$$F_i(0) = 0. \tag{29}$$

For realization of the conditions of (29), it is necessary to begin numerical integration with $r = 0$ and at the same time to choose the solution regular in zero.

At $r \to 0$ system (7) can be replaced by the equations

$$\left[\frac{d^2}{dr^2} - \frac{l_i(l_i+1)}{r^2} + \frac{2Z}{r}\right] F_i(r) = 0, \quad i = 1,2,3. \tag{30}$$

The solution of (30) is found in the form of a series

$$F_{il}(r) = a_i r^{l_i+1} \sum_{n=0}^{\infty} \frac{1}{n!} \cdot \frac{(2l_i+1)!}{(2l_i+1+n)!}(-2Zr)^n. \tag{31}$$

Series (31) was used in order to begin numerical integration close to zero.

From expression (18) for G_{ij} it follows that the system of equations contains integrals of the type $\int_0^r$ and $\int_r^{\infty}$. Substituting $\int_r^{\infty} = \int_0^{\infty} -$ system (7) can be rewritten in the form

$$\sum_i L_{ij} F_j(r) = \pm \sum_{jn} D_{ijn} M_{jn}(r) \int_0^{\infty} N_{nj}(r') F_j(r') dr', \tag{32}$$

where L_{ij} is an integro-differential operator containing integrals of the type $\int_0^r$.

Computation of the cross section $n_0s - n_0p$ of excitation for Li, and Cs in reference [30] was carried out analogously to the computation for Na in [29]*. In [30] the sum of the elastic and $n_0s - n_0p$ cross sections for Li, Na, K and Cs at energies up to 50 eV was also calculated. The sum of the elastic and inelastic cross sections was practic equal to the full cross section, since the excitation cross sections of the upper levels were much less. The sum seemed close to the experimental data.

In reference [31] other modifications of Born's approximation [32,33] were used, in which the Born matrix elements relate, not to the transition matrix (T-matrix), but to the reaction matrix (K-matrix) or to the proper phase of the scattering matrix. The T-matrix is then calculated from them. Such methods of calculation ensure observance of the theoretical limit for partial cross sections. We note that in these articles the K-matrix is designated by the letter R, which is not entirely suitable, since it could be confused with Wigner's R-matrix.

The modifications in perturbation theory shown in [31] were applied to Bethe's approximation (in interaction potentials only terms of the type $C r^{-2}$ were taken into consideration).

The computation was carried out for elastic scattering and for $n_0s - n$ excitation of Na and Cs by electrons at energies up to 100 eV. Elastic scattering is wholly caused by the presence of real inelastic processes, and it disappears at energies below the threshold of excitation.

The results obtained in [26] for excitation of Na by the distorted wave approximation and without exchange were evaluated in reference [34] by a method in which the calculated matrix elements are analogous to the K-matrix. This significantly improved agreement with experimental data.

In [24] this method was used to calculate $\sigma(3s - 3p)$ for Na, also the usual Born approximation, which decreased the cross section significant We note that this method of computation is often called calculating the str coupling by the Born approximation. The name refers to the fact that durin calculation of the amplitude of transition for one process, the matrix elem of other processes are also used.

In a much later reference [35] a system of equations analogous to (7), but taking into consideration only long-range dipolar terms, was solved in the following manner. In the first approximation it was understood that k (this condition in [35], just as in [21], is called resonance). Then the system of equations is solved analytically by known functions. The F_1 ob is further substituted into the equation for F_2 and F_3, which are then solved without difficulty. The numerical computation in [35] was carried o for 3s - 3p excitation of Na.

It may be noted that on the whole the methods which consider only the long-range potentials give comparatively closer results. Their application valid for those energies at which a basic contribution to the effective cro section is made by partial cross sections corresponding to large momentum o the incident electron, for which exchange and other short-range forces are immaterial.

* Cross sections of excitation of Cs were also calculated by this approxi in reference [66].

By the same approximation as in the present article, i.e., with calculation of exchange and of the $n_0s - n_0p$ strong coupling, effective cross sections of elastic scattering and excitation of lithium by electrons at energies of 2-3 eV were found [36] by numerical solution of equation (7). In [3] scattering lengths of electrons on sodium were calculated by a similar approximation.

The so-called exchange-polarization approximation is a simplified variant of the system of equations (7), in which polarization is usually considered as an adiabatic approximation. During determination of deformation of the atom, the incident electron is considered as a stationary center of force. If, however, polarization of the atom is determined by first order perturbation theory, then the distorted functions F_2 and F_3 are expressed in terms of F_1 [37]:

$$F_2 \quad \frac{V_{12}}{\varepsilon_2-\varepsilon_1}F_1; \quad F_3=-\frac{V_{13}}{\varepsilon_3-\varepsilon_1}F_1. \qquad (26)$$

The equation for elastic scattering which we obtain by substituting (26) into (7) and considering only dipolar members in the exchange-polarization part (G_{12}, G_{13}) was solved for lithium in reference [38]. The authors of reference [39] examined electron scattering on cesium atoms by the same approximation, but completely neglecting potentials G_{12} and G_{13}. In [39] the computation was also carried out in another variant of the adiabatic approximation, in which polarization of the atom was determined by the variation method.

A comparison of the partial cross sections calculated in references [36, 38] shows that substitution of (26) is not satisfactory at energies exceeding the threshold of excitation. The applicability of the adiabatic approximation at energies below the excitation threshold is discussed in [40].

Simpler approximations, in which exchange is not considered and the polarized potential is determined by semi-empirical means, are used in references [41, 42, 67] in regard to elastic scattering on Cs, Na and K.

In conclusion, we mention reference [43], in which only short-range correlations of the incident electron and the atomic electrons are considered, but nevertheless comparatively large effective cross sections were obtained at low energies (on the order of experimental cross sections), although as energy increased the calculated cross sections decreased too quickly. The last agrees with the results of investigations [41, 42] into the role of long-range interactions.

METHODS OF COMPUTATION

The methods of solving integro-differential equations are divided into two groups: iterative and non-iterative. Iterative methods were used in references [44 - 46] but, as is seen from these articles, iterations do not always converge well. The present article uses the non-iterative method of Marriott and Percival, first proposed in Marriott's article [47]. This method was used in references [48, 49]. We note that the non-iterative method proposed earlier by Drukarev [50] was in essence close to the Marriott-Percival method.

It is necessary to set apart the case in which a system of equations is integrated only from r = 0 or from both zero and large distances, and the solutions are joined at an intermediate point. Here we set forth the method for the case where integration proceeds only from zero. The methods of soluti for integration with two limits are set forth in [40].

We note that, in contrast to the case of elastic scattering, in which both in Born's approximation and in the distorted waves method the decreasing static potential falls off rapidly, the transition matrix element contains a slowly decreasing ($\sim r^{-2}$) potential in both approximations for excitation of the n_0p state, and therefore higher partial cross sections follow.

Seaton [29] applied the following variation of Born's approximation:

1. In the Born matrix element, in potential $n_0s - n_0p$ of an interaction, only a term of the type $C r^{-2}$ is considered, which corresponds to substituting Bethe's approximation for Born's approximation, and the necessity for having atomic wave functions no longer arises, since at r^{-2} the coefficient is expressed through the oscillator strength, which can be taken from experimental data.

2. For those partial cross sections for which Bethe's approximation gives more than half of the theoretical limit, half of the theoretical limit is taken as the result.

The results of such a semistatistical method seem significantly nearer experimental results than those of the ordinary Born approximation. In reference [29] the $3s - 3p$ excitation in Na was examined by such a method at energies up to 50 eV.

An analysis of the so-called schematic model which serves to substantiate the modified Born approximation is shown in [29] - a system of equations:

$$(\Delta + k_1^2) F_1 = \frac{A}{r^2} F_2; \qquad (\Delta + k_2^2) F_2 = \frac{A}{r^2} F_1, \tag{25}$$

reflecting the basic features of the strong $n_0s - n_0p$ coupling.

System (25) has an exact solution in known functions, if $k_1 = k_2$.

Postulating in (25) that $k_1 = k_2$ and using an exact solution, the authors of reference [30] calculated the effective cross section of elastic scattering of electrons on Li, Na, K and Cs, determining A as

$$A = \frac{4}{\pi \sqrt[3]{3}} \gamma \overline{S},$$

where S is the line strength for the $n_0s - n_0p$ transition.

We note that elastic scattering in the schematic model is of a polarized nature, i.e. it is caused by the presence of virtual and real inelastic processes, and together with the inelastic cross section it disappears at $A \to 0$.

The solution of the schematic model at $k_1 = k_2$ has a physical meaning, if $2l + 1 > 2\sqrt{A}$. At lesser l the partial cross sections in [30] were estimated as in [29] - half the theoretical limit.

The method of calculation applied to elastic scattering in [30] is inapplicable to inelastic scattering, since the sum of the inelastic partial cross sections according to l in the schematic model diverges logarithmically at $k_1 = k_2$.

$$F_i \to F_i + \alpha_{i1} u_1 + \alpha_{i2} u_2 + \alpha_{i3} u_3. \tag{23}$$

According to (22), these can differ from zero

$$\begin{aligned} &\text{at} \quad L = 0 \quad \alpha_{11}^-; \quad \alpha_{33}^-; \\ &\text{at} \quad L = 1 \quad \alpha_{12}^- = -\alpha_{21}^+; \quad \alpha_{13}^- = \alpha_{31}^-; \\ &\text{at} \quad L = 2 \quad \alpha_{32}^-. \end{aligned} \tag{24}$$

REVIEW OF THEORETICAL METHODS

One of the simplest methods is Born's approximation. The cross section $\sigma(2s - 2p)$ for Li is calculated by this approximation in [22], and the data on excitation of Na are introduced in [23, 24]. Tables 8 and 9 show Born cross sections of elastic scattering and excitation of the n_0p level of the alkali metals by electrons, as calculated in the present article. For Na the Born cross section $\sigma(3s - 3p)$ has a maximum more than twice that of the experimental. The experimental cross section of excitation of the resonance lines of potassium [13] has a maximum equal to 150 πa_0^2 at energies of 5 - 6 while that of Born's approximation has 191 πa_0^2 at 3 eV. Experimental data for excitation of Li are unknown. The relative cross section for Cs has been measured [10, 11]; it has a gently sloping maximum at 7 eV. Born's approximation gives a maximum at 2.75 - 3 eV.

At low energies the Born elastic cross section for Li and Na is close to the experimental cross section, but for K and Cs it is significantly greater. A detailed analysis of Born's partial cross sections of elastic scattering on Li is given in reference [25]. It appears that the cross section for the s-wave exceeds the theoretical limit, while cross sections for higher waves are too low. Born's approximation does not take into consider tion deformation of the atom by the incident electron, which is important in alkali metals. Furthermore, the static potential of these atoms is so high that the perturbation theory is inapplicable.

In [26] the excitation cross section of Na is calculated by numerical integration of the equations in the distorted waves approximation, without exchange. It seems greater than the Born one. Several partial cross sections exceeded the theoretical limit. The full cross section had three maxima. Exchange calculation within the limits of this same approximation decreased th cross section significantly [24]. In the first approximation of the integral equation method, the distorted waves equations for excitation of Na were solve in [27], while those for elastic scattering on Li were solved in reference [28].

At $L > 0$, system (32) contains three equations and nine different integrals:

$$N_{nj} \equiv \int_0^\infty N_{nj}(r) F_j(r) dr. \qquad (33)$$

A full set of linearly independent solutions of system (32) can be constructed from the three linearly independent solutions of the homogeneous system of equations

$$\sum_{q} \ldots F_{\ldots}^{(pq)}(r) = 0, \quad p = 1, 2, 3 \qquad (34)$$

and the nine solutions of the system, in which one of the integrals N_{nj} is replaced by some constant $\ldots_{nj}$, but the remaining ones by zeros:

$$\sum_{} \ldots F_{\ldots}^{(pq)}(r) = \pm D_{(pq} M_{pq}(r) \alpha_{pq}. \qquad (35)$$

The unknown solution is represented in the form of a linear combination

$$F_{\ldots} = \sum_{pq} C^{(pq)} F_{\ldots}^{(pq)}, \quad \begin{matrix} p = 1, 2, 3, \\ q = 0, 1, 2, 3. \end{matrix} \qquad (36)$$

Substituting (36) into (32), considering (34) and (35), and equating the multipliers with separate functions $M_{ij}(r)$, we get a system from the nine algebraic equations:

$$\sum_{pq} C^{(pq)} \left[\int_0^\infty N_{ij}(r) F_j^{(pq)}(r) dr - \delta_{ij,pq} \alpha_{pq} \right] = 0, \quad ij = 11, 12, \ldots 33. \qquad (37)$$

Since the number of unknown coefficients $C^{(pq)}$ is equal to 12, three additional conditions can be imposed.

We require that F_i have a determinate behavior near zero

$$F_i(r) \sim b_i r^{l+1}. \qquad (38)$$

Supposing that

$$F_i^{(pq)}(r) \sim a_i^{(pq)} r^{l+1}, \qquad (39)$$

we get three additional equations

$$\sum_{pq} C^{(pq)} a_i^{(pq)} = b_i, \quad i = 1, 2, 3. \qquad (40)$$

Three linearly independent solutions can be obtained by varying b_i.

For unknown integrals we get the expression

$$\int_0^\infty N_{\ldots}(r) F_i(r) dr = \ldots_i C^{(pq)}. \qquad (41)$$

Functions N_{ij} ... decrease comparatively quickly, and therefore with the exchange calculation ... seems sufficient to integrate the system of equations up to $r = 27$ atomic units. The interval of integration changes from 0.005 up to 0.16 atomic units. Numerical integration was carried out by method X1 according to [51] with ... evaluation. Integrals were calculated according to Simpson's formula.

After determination of exact integrals of N_{ij} according to formula (41), system (32) was solved once again with them. The integration was carried out up to $r = 150$, where the elements of the K-matrix were determined with the aid of asymptotic series [44, 52].

For $L = 0$ a system of two equations, containing five different integrals was solved.

At $L \geq 2$ the accuracy of the computation during integration seems unsatisfactory only from zero. The requirement of symmetry of $K_{ij} = K_{ji}$ is poorly fulfilled. The reason, apparently, is that errors of integration increase more rapidly with increase of distance than linearly. Therefore at $L \geq 2$ the computation was mainly carried out by means of integration with two limits. For this we contrived a program which carried out this computation for energies below the excitation threshold [40]. We note that this program also used another formula of numerical integration - Vozheler's method. More convenient methods for this computation are set forth in reference [40]. All computations were carried out on the BESM-2M at the P. Stuchka Latvian State University Computer Center.

RESULTS

Computations in the present article were carried out at incident electron energies

$$E_r < E \leq 5 \text{ eV},$$

where E_r is the resonance potential (excitation threshold of the n_0p level).

We used semi-empirical wave functions for Na, K and Cs [15]. The potential due to the filled shells was determined by Gaspar's method [53].

Hartree-Fock wave functions without full self-consistency (i.e., without calculation of the effect of the valence electron on the core) were used for Li. The authors of reference [14] were kind enough to give us their numerical results.

Such functions were first calculated by means of numerical integration in reference [54]. The authors of reference [14] calculated these functions with the aid of an electronic computing machine, and used them in the capacity of an initial approximation for computation of atomic functions of Li with full self-consistency.

The resonance potentials E_r, corresponding to the atomic functions of Li, Na, K and Cs that we used, equal:

	Li	Na	K	Cs
E_r, eV	1.84	2.10	1.61	1.42

At energies above the excitation threshold of the n_0p level, the effective cross sections are determined through elements of the T-matrix.

The total cross section of elastic scattering

$$Q_0 = 2\pi \int_0^\pi I(\theta) \sin\theta d\theta = \frac{\pi}{k^2} \sum_L (2L+1)|T_{11}^{(L)}|^2, \tag{42}$$

where $I(\theta)$ is the differential cross section of elastic scattering.

The total cross section of excitation of the n_0p level

$$Q_{n_0p} = \frac{\pi}{k^2} \sum_L (2L+1)[|T_{12}^{(L)}|^2 + |T_{13}^{(L)}|^2]. \tag{43}$$

The total cross section of scattering equals

$$Q = Q_0 + Q_{n_0p} \tag{44}$$

The effective cross sections of diffusion and viscosity equal:

$$Q^{(1)} = 2\pi \int_0^\pi I(\theta)(1-\cos\theta)\sin\theta d\theta = \frac{\pi}{k^2} \sum_L (L+1)|T_{11}^{(L)} - T_{11}^{(L+1)}|^2, \tag{45}$$

$$Q^{(2)} = 2\pi \int_0^\pi I(\theta)(1-\cos^2\theta)\sin\theta d\theta = \frac{\pi}{k^2} \sum_L \frac{(L+1)(L+2)}{2L+3}|T_{11}^{(L)} - T_{11}^{(L+2)}|^2. \tag{46}$$

Below the excitation threshold, T_{11} is expressed through the phase of the elastic scattering:

$$T_{11} = -2ie^{i\eta}\sin\eta. \tag{47}$$

The differential cross section of elastic scattering can be written in the form

$$I(\theta) = \frac{1}{4k^2}\left|\sum_L (2L+1)T_{11}^{(L)}P_L(\cos\theta)\right|^2. \tag{48}$$

The transition matrices of the direct and exchange scattering are determined through the matrices of the singlet (+) and triplet (-) cases:

$$T_{dir} = \frac{1}{2}[T^+ + T^-];$$

$$T_{exch} = \frac{1}{2}[T^+ - T^-]. \tag{49}$$

During exchange calculation, cross sections (42 - 46) were averaged according to spin and summed.

Total effective cross sections of collision of electrons with atoms of Li, Na, K and Cs, calculated by the approximation of strong coupling, are shown in Table 2.

During calculation of total cross sections, all nine partial waves (L = 0,1, . . . , 8) were considered.

At L = 4 for Li, Na and K, the spin-averaged partial cross sections are practically equal to the cross sections obtained without exchange. Therefore for Li, Na and K up to L = 3 the spin-averaged cross sections are summed, but for higher waves ($L \geq 4$) non-exchange cross sections were used. For Cs exchange was considered for $L \leq 4$.

Tables 3 - 6 show partial cross sections of elastic scattering and excitation of the n_0p level for the singlet (+) and triplet (-) cases, without exchange. The singlet and triplet cross sections are averaged according to spin, i.e., given singlet cross sections are multiplied by 1/4, and triplet by 3/4.

In order to evaluate the effect of the choice of atomic functions, in the present article the computation of cross sections is also carried out with atomic functions corresponding to Stone's potential for Cs at several energies. This potential was so constructed in reference [47] that the difference between theoretical and experimental values of the energy levels and oscillator strengths were minimal. Using Stone's potential, we calculated the eigenfunctions 6s and 6p of the states of a cesium atom without calculating spin-orbital interactions.

Table 7 shows partial cross sections of elastic scattering and excitation of the 6p level of a Cs atom, calculated with Stone's wave functions. The full cross section of scattering, calculated at 2 eV, increased 12% ($283\ a_0^2$ instead of 258). Additional computations for separate partial cross sections showed that the dependence of these cross sections upon energy did not vary qualitatively.

"The perfect scattering experiment"

What is the best you can do, i.e., what must be done to extract the most information possible from a scattering experiment? If the electron is structureless then the only parameters that describe the scattering are:

elastic : phase shift, or, a 1×1 S-matrix - only energy and angle specific measurements required

inelastic $s \to p$ (no spin-orbit interaction)

T_{12}, T_{13} (or T_{21}, T_{31}): two complex numbers at each energy, angle. i.e., 4 parameters. However, as with all wavefunctions one phase is undeterminate, so there are 3 parameters required

elastic with spin : $S^{\pm}$ i.e., three

inelastic with spin : $T^{\pm}_{12}, T^{\pm}_{13}$ i.e. seven

inelastic with spin and with magnetic interaction : fifteen.

Apart from the ability to prepare the atom in an excited state, for $p \to p$, $p \to d$ etc scattering, the laser also can be used to prepare the time-inverse S-P collision; in fact, it is a better way to study inelastic processes than the other competitive method (e; e, 2e): coincidence experiments, We'll see this later.

It is crucial, in understanding how to deal with such experiments (a) to deal properly with the time hierarchy and (b) to keep accurate track of appropriate quantization axes.

(a) time hierarchy

t_{coll} : collision time (potential scattering) $\sim 10^{-15} - 10^{-16}$ sec

t_{s-o} : spin orbit relaxation time ($LM_L, SM_S \to \mathcal{J}, J, M_J$) [i.e., fine structure] $\sim 10^{-12} - 10^{-13}$ sec

t_{hfs} hyperfine structure relaxation time [nuclear moments] $\sim 10^{-9} - 10^{-10}$ sec

$1/\Omega$ Rabi frequency $\sim 10^{-7} - 10^{-9}$ sec for single mode cw lasers

τ radiative lifetime $\sim 10^{-7}$ sec

t_a : time spent by atom in interaction region $\sim 10^{-5}$ sec

Axes of quantization

As already indicated, the axis of choice for computation is along the electron's incoming momentum. Then

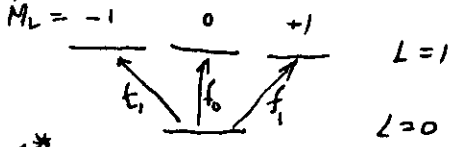

$f_{-1} = f_1^*$

because ground state is spherically symmetric:

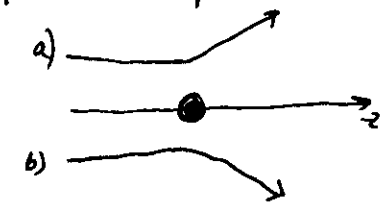

a) & b) will (must) excite atom identically, which means that excited electron must rotate in opposite senses

In recent alignment & orientation work, Hertel, Andersen and others have favored the so-called "natural" quantization axis, perpendicular to the plane of scattering since [see below] f_0 will be zero along that direction.

I now include the first few pages of review article by Andersen, Gallagher and Hertel which gives an excellent overview of the quantization picture:

XIV ICPEAC, Pub Alb, Invited paper (1986)

ALIGNMENT AND ORIENTATION OF ATOMIC OUTER SHELLS INDUCED BY ELECTRON AND ION IMPACT: SOME RECENT DEVELOPMENTS AND REMAINING PROBLEMS

Nils ANDERSEN,* Jean W. GALLAGHER and Ingolf V. HERTEL†

Joint Institute for Laboratory Astrophysics, National Bureau of Standards and University of Colorado, Boulder, Colorado 80309 USA

Alignment and orientation of atoms in collision experiments with planar symmetry have now been studied for about 15 years and close to 500 papers have been produced, mainly devoted to S→P excitation. Despite the large variety of electron-atom, ion-atom and atom-atom collision systems considered, a unified framework for description of these phenomena is now emerging. This framework is a generalization of the original ideas of Macek and Jaecks and is based on consideration of symmetries, conservation laws, etc. The key parameters are directly related to the shape and dynamics of the charge cloud of the excited electron as well as to experimental observables. A brief review is given of this framework, and some current problems and prospects for the future are discussed.

1. INTRODUCTION

The field of alignment and orientation in atomic collisions is devoted to the study of the shape and dynamics of the electronic charge clouds excited in a collision process. Obviously this kind of information, most effectively obtained from experiments with planar symmetry, provides a much more severe test of our understanding of the excitation mechanisms than determination of, say, a probability or a cross section for excitation. As will be detailed below, in favorable cases a complete determination of the quantum-mechanical state of the system may be obtained, thereby providing a so-called "perfect scattering experiment," the most fundamental level at which experiment and theory can be compared. The shape and dynamics are expressible in dimensionless parameters based on relative measurements, thereby eliminating the otherwise often serious problem of accurate determination of absolute units. Furthermore, they may be very sensitive to details in the theoretical description in cases where the cross sections show only minor variations.

At previous ICPEAC's several symposia (1,2) review papers (3,4) and progress reports (5), and a large number of contributed papers have dealt with various particular aspects of this field. The Data Center of the Joint Institute for Laboratory Astrophysics is currently undertaking a critical review of this whole flourishing field, restricted to excitation of outer shells of atoms in planar scattering experiments using unpolarized beams. During this review several parallel lines of thought within the otherwise traditionally separated fields of electron-atom and atom-atom collisions became evident. In particular a unified framework, or language for description of these phenomena, is developing though several "local dialects" still exist and probably will persist, partly due to differences in nature of the underlying physics for specific problems. Below we shall first try to summarize this framework, mainly concentrating on S→P excitation to which about 95% of the literature is devoted. Then some selected current problems will be discussed within this framework and conclusions drawn concerning areas where future efforts might be most fruitfully concentrated. The discussion will be restricted to excitation of states decaying by photon emission, though most of the ideas can be easily modified to include electron emission as well, cf. Niehaus (6).

2. FRAMEWORK

2.1. Coordinate frames, basis functions, symmetries and time scales

In an experiment, the collision plane is determined by e.g. the two directions of incoming and outgoing particles, thereby fixing the scattering angle. Excitation processes corresponding to this scattering angle are then studied by analysis of either the polarization properties or the angular distribution of the secondary photons emitted when the excited state decays, detected in coincidence with the scattered particle, or, in time reversed experiments, analysis of the scattered particles as function of the polarization properties of the laser light used to prepare the target atoms prior to the collision. These procedures are detailed in recent reviews (7-9), so we shall just briefly outline the principles here.

Since the symmetry properties of the force(s) determining the excitation and time evolution of the charge cloud will be seen to play an essential role, we shall recall the symmetry properties of the three eigenstates corresponding to a P-level, neglecting at first the effect of fine and hyperfine structure, which will be included later. The upper panel of Fig. 1 shows the angular parts of the charge clouds for the so-called "atomic physics basis" ($|p_{+1}\rangle$, $|p_{-1}\rangle$, $|p_0\rangle$), with $|p_M\rangle$ labelled according to the magnetic quantum number M. Here we quantize along the axis perpendicular to the collision plane since this choice simplifies the subsequent mathematical description considerably. The lower panel of Fig. 1 shows the alternative "molecular physics basis" corresponding to real-valued wave functions ($|p_x\rangle$, $|p_y\rangle$, $|p_z\rangle$), describing p-orbitals along the three coordinate axes. The state $|p_0\rangle = |p_z\rangle$ has negative reflection symmetry with respect to this plane, while the other ones have positive reflection symmetry.

Notation for circularly polarized light varies in the literature. We here use the definition of classical optics (1D), which uses the term left handcircularly (LHC) polarized light, if the electric vector is seen to rotate counter-clockwise when looking toward the light source, i.e. LHC-photons have positive helicity. Referring to Fig. 1, decay of the state $|p_{+1}\rangle$ will thus lead to emission of LHC-photons in the +z (RHC-photons in the -z) direction.

At this point it is useful to recall some important time scales:

(i) τ_c, the collision time, during which the excitation takes place; $\tau_c \sim a/v$, where a is a characteristic interaction length and v the collision velocity.

(ii) τ_{fs}, the characteristic time for the fine structure; $\tau_{fs} \sim 1/\omega_{fs}$, where $\hbar\omega_{fs}$ is the fine structure splitting.

(iii) τ_{hfs}, the characteristic time for the hyperfine structure; $\tau_{hfs} \sim 1/\omega_{hfs}$, where $\hbar\omega_{hfs}$ is the hyperfine structure splitting.

(iv) τ_{nat}, the (natural) lifetime; $\tau \sim 1/A$, where A is the decay probability.

(v) τ_{obs}, the observation time for an atom in the actual experimental setup.

Each specific situation requires consideration of these magnitudes. An atom that is initially in an S state has positive reflection symmetry.

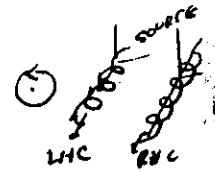

*Permanent address: Physics Laboratory II, H.C. Ørsted Institute, DK-2100 Copenhagen, and Institute of Physics, University of Aarhus, DK-8000 Aarhus, Denmark.

†Permanent address: Institut für Molekülphysik, Fachbereich Physik, Freie Universität Berlin, Arnimallee 14, D-1000 Berlin 33, West Germany.

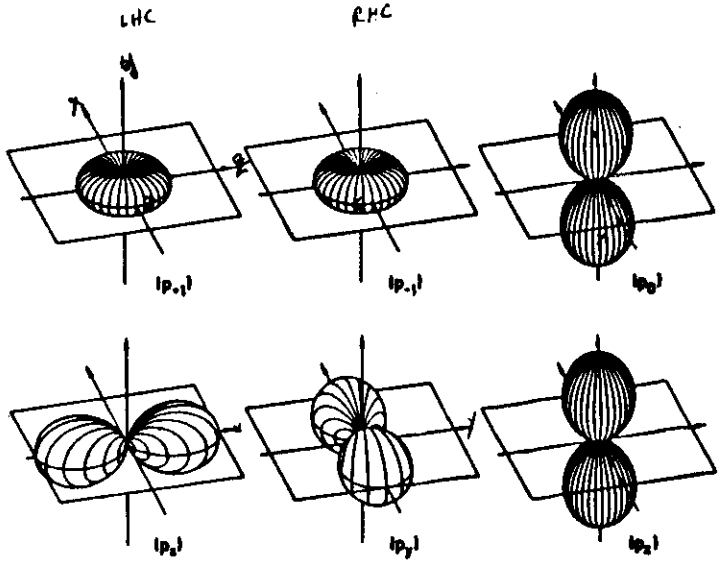

FIGURE 1

The total wave function describing the collision event conserves its reflection symmetry with respect to the scattering plane. Often fine and hyperfine forces are so weak, they can be neglected during the collision so that the excitation is caused by Coulomb interaction only. In the simple case where the collision partner acts as a spinless, structureless particle, this implies that the (spatial part of the) wave function of the atom that is excited preserves its reflection symmetry during the collision. Thus excitation to a P-level can only take place to two of the three states of Fig. 1: "Out-of-plane" excitation of $|p_z\rangle$ is forbidden.

After the collision the isolated, excited atom may develop further under the influence of the fine structure (and possibly hyperfine structure) force, which does not conserve reflection symmetry of the spatial part of the wave function, thereby allowing the charge cloud to change shape in time until the decay takes place. We shall treat these two regimes -- excitation and time development -- separately, and see how it is possible to reconstruct the nascent charge cloud, the object of interest to collision physics, from the actual observed radiation pattern and a knowledge of τ_{fs}, τ_{hfs}, τ_{nat} and τ_{obs}.

2.2. S→P excitation

2.2.1. The simplest case: Full coherence -- the Poincaré sphere

We shall first analyze the properties of the radiation pattern in the simplest case in which the excited P-level of the atom can be described by a state vector, i.e. its coordinates (a_{+1}, a_{-1}, a_0) in the basis of Fig. 1. Reflection symmetry conservation implies $a_0 = 0$. This situation may be encountered in, e.g., electron impact excitation of a He(n^1P) level.

Figure 2(a) shows an example of the angular part of the P-state electron density. Three coordinate frames are shown: (i) the collision frame (x^C,y^C,

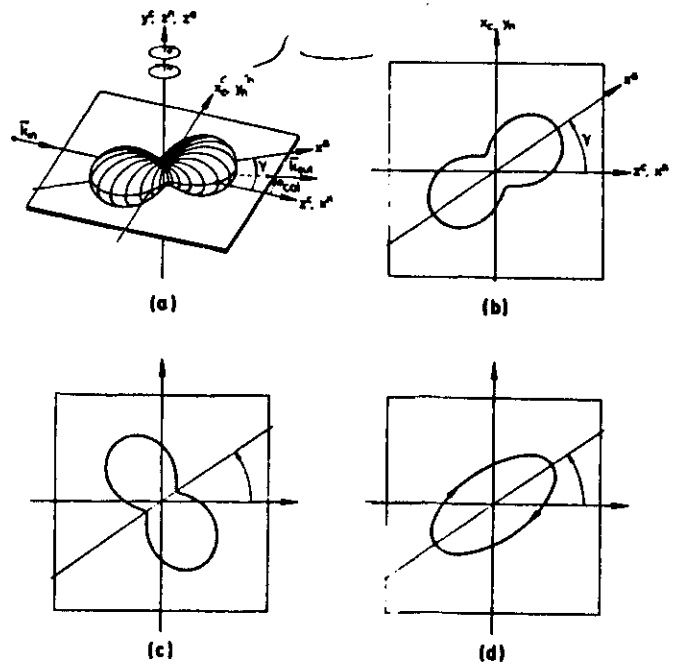

FIGURE 2

z^C) with z^C in the direction $\hat{k}_{in}$ of the incident particles, (x^C,z^C) is the collision plane, and y^C is parallel to $\hat{k}_{in} \times \hat{k}_{out}$. ϑ_{col} is the scattering angle; (ii) the natural frame (x^n,y^n,z^n) with $x^n = z^C$, $y^n = x^C$, $z^n = y^C$; finally, another convenient frame (iii) is the atomic frame (x^a,y^a,z^a) obtained from the natural frame by rotation through an angle γ around $z^n = z^a$ so that x^a parallels the major symmetry axis of the charge cloud, which is also a symmetry axis for the radiation pattern. Assuming normalization, $a_{+1}^2 + a_{-1}^2 = 1$, then, apart from an arbitrary common phase factor, the wave function is completely characterized by the two parameters (γ,$L_\perp$), where γ is the alignment angle and $L_\perp^2 = a_{+1}^2 - a_{-1}^2$ is the angular momentum pointing along z^n. In the atomic frame the wave function takes the simple form

$$|\psi\rangle^a = 2^{-1/2}\left[(1+L_\perp)^{1/2}|p_{+1}\rangle^a - (1-L_\perp)^{1/2}|p_{-1}\rangle^a\right] \quad . \qquad (1)$$

Using polar coordinates (θ,ϕ) in the natural frame, the angular part T of the charge cloud may be written as (omitting a $3/4\pi$ normalization factor)

$$T(\theta,\phi) = \tfrac{1}{2}\,[1+P_\perp \cos 2(\phi-\gamma)]\sin^2\theta \quad . \qquad (2)$$

Figure 2(b) shows a cut through the charge cloud in the collision plane, given by

$$T(\tfrac{\pi}{2},\phi) = \tfrac{1}{2}\,[1 + P_\perp \cos 2(\phi-\gamma)] \quad . \qquad (3)$$

$P_\perp$, the linear polarization, is thus a width parameter, with $(1+P_\perp)/2$ and $(1-P_\perp)/2$ determining the major and minor axes of the charge cloud in the collision plane.

The angular correlation pattern of the photons emitted from the excited atoms and detected in the collision plane is given by ($\theta = \pi/2$)

$$I(\phi) = 1 - P_\perp \cos 2(\phi-\gamma) \quad . \qquad (4)$$

This pattern, Fig. 2(c), is thus identical to the shape of the charge cloud, Eq. (3) and Fig. 2(b), rotated by 90°, as expected from the properties of electric dipole radiation.

Alternatively one may measure the polarization ellipse observed in the $+z^n$ direction with a linear and circular polarizer, Fig. 2(d), or equivalently, the three Stokes parameters (P_1,P_2,P_3) defined by

$$1\cdot P_1 = I(0°) - I(90°)$$

$$1\cdot P_2 = I(45°) - I(135°)$$

$$1\cdot P_3 = I(RHC) - I(LHC)$$

where I is the total light intensity in the z^n direction, and $I(\theta)$ is the light transmitted through an ideal linear polarizer tilted at an angle θ with respect to x^n [sometimes one may find the alternative notation $(n_1,n_2,n_3) = (P_2,-P_3,P_1)$]. Evidently

$$\vec{P} = (P_1,P_2,P_3) = (P_\perp \cos 2\gamma,\ P_\perp \sin 2\gamma,\ -L_\perp) \qquad (5)$$

with the linear polarization $P_\perp = (P_1^2+P_2^2)^{1/2}$ being invariant under rotation around z^n. Furthermore, the light emitted is fully coherent, such that the degree of polarization

$$P = |\vec{P}| = (P_1^2+P_2^2+P_3^2)^{1/2} = (P_\perp^2+L_\perp^2)^{1/2} \qquad (6)$$

in this case is unity, and $P_\perp$ thus fully determined from $L_\perp$.

The Stokes vector (P_4,P_5,P_6) measured in the y^n direction is (1,0,0) and adds no further information in this case.

A correlation experiment, Fig. 2(c), determines $(\gamma,P_\perp)$ while a coherence experiment, Fig. 2(d), determines $(\gamma,L_\perp)$. Thus, here, a coherence experiment is a "perfect scattering experiment" in the sense discussed in the introduction, while a correlation experiment only determines $P_\perp$, leaving the sign of $L_\perp$ undetermined. The parameters used in Fig. 2 are $\gamma=35°$, $L_\perp=0.8$ and $P_\perp=0.6$.

For later generalization we also state the density matrix $\rho_{mn} = a_m a^*_n$ in the natural frame (tr ρ=1)

$$\begin{Bmatrix} \rho^n_{11} & 0 & \rho^n_{1-1} \\ 0 & \rho^n_{00} & 0 \\ \rho^n_{-11} & 0 & \rho^n_{-1-1} \end{Bmatrix} = \frac{1}{2}\begin{Bmatrix} 1-P_3 & 0 & -P_1+iP_2 \\ 0 & 0 & 0 \\ -P_1-iP_2 & 0 & 1+P_3 \end{Bmatrix} \quad . \qquad (7)$$

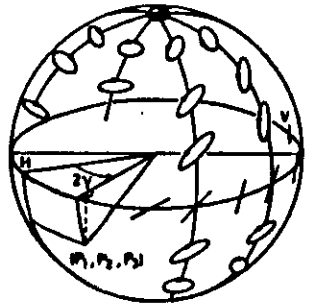

FIGURE 3

A succint way of summarizing this situation is by introducing the Poincare sphere (11), making use of the fact that the point $\vec{P} = (P_1,P_2,P_3)$ is located on a unit sphere, cf. Eq. (6). Figure 3 illustrates the polarization ellipse corresponding to various points on the sphere, with H=(1,0,0) corresponding to $|p_x\rangle$ or horizontal linear polarization in Fig. 2(d), V=(-1,0,0) corresponding to $|p_y\rangle$ or vertical linear polarization, the north pole to $|p_{+1}\rangle$, and the south pole to $|p_{-1}\rangle$. Two opposite points on the sphere correspond to orthogonal states. In this language, a coherence experiment determines a point on the Poincare sphere, while a correlation experiment only determines its projection on the equatorial plane, $P_1+iP_2 = P_\perp e^{2i\gamma} = -2\cdot\rho^n_{11}$.

2.2.2. Loss of full coherence

Where several processes which are in principle distinguishable contribute, the excitation may no longer be coherent. For instance, in the low energy electron impact excitation of a $H(n^2P)$ level, exchange effects lead to different amplitudes for singlet and triplet scattering, and if no spin analysis is performed before or after the collision the corresponding density matrix elements have to be added incoherently. This situation can no longer be represented by a wave function. Positive reflection symmetry is still conserved. The light emitted in the $+z^n$ direction is no longer fully coherent so that $P<1$. All Eqs. (2)-(7) remain valid. However, $P_\perp$ and $L_\perp=-P_3$ are now independent parameters. Thus, in this case three parameters are needed to specify the situation completely, namely $(\gamma,L_\perp,P_\perp)$. A correlation experiment only determines shape $(P_\perp)$ and alignment angle γ, but gives no information about dynamics $(L_\perp)$, while coherence analysis still provides complete information.

2.2.3. The general case

In the general case the assumption for the atomic wave function of positive reflection symmetry only cannot be maintained. This may happen, for example, in electron impact excitation of P levels of the heavy rare gases for which spin-orbit effects are so strong that they play a role during the collision ($\tau_{fs}\sim\tau_c$), at least at low energies. Equation (7) must then be replaced by

$$\begin{Bmatrix} \rho^n_{11} & 0 & \rho^n_{1-1} \\ 0 & \rho^n_{00} & \\ \rho^n_{-11} & 0 & \rho^n_{-1-1} \end{Bmatrix} = (1-\rho^n_{00})\,\frac{1}{2}\begin{Bmatrix} 1-P_3 & 0 & -P_1+iP_2 \\ 0 & 0 & 0 \\ -P_1-iP_2 & 0 & 1+P_3 \end{Bmatrix} + \rho^n_{00}\begin{Bmatrix} 0 & 0 & 0 \\ 0 & 1 & 0 \\ 0 & 0 & 0 \end{Bmatrix}. \qquad (8)$$

Equation (8) shows the decomposition of the density matrix into two parts, one having positive and one negative reflection symmetry. While Eq. (5) still holds, Eq. (2) is replaced by

$$W(\theta,\phi) = (1-\rho_{00})\,\tfrac{1}{2}\,[1+P_\xi\cdot\cos 2(\phi-\gamma)]\cdot\sin^2\theta + \rho_{00}\cdot\cos^2\theta \quad . \qquad (9)$$

ρ_{00} is thus a height parameter, the determination of which requires observation from a direction different from z^n. Here and below we abbreviate $\rho_{00} = \rho^0_{00} = \rho^1_{00}$. Within the positive reflection symmetry we define explicitly $P_\perp{}^+ = (P_1{}^2+P_2{}^2)^{1/2}$, $L_\perp{}^+ = -P_3$ and $P^+ = (P_1{}^2+P_2{}^2+P_3{}^2)^{1/2} = (P_\perp{}^2+L_\perp{}^2)^{1/2}$. In the y^n direction the Stokes parameters are now $(P_\xi,0,0)$ with $P_\xi<1$. Then

$$\rho_{00} = \frac{(1+P_\perp)(1-P_\xi)}{4-(1-P_\perp)(1-P_\xi)} \quad . \qquad (10)$$

The angular momentum is given by

$$L_\perp = -P_3(1-\rho_{00}) = L_\perp{}^+(1-\rho_{00}) \quad . \qquad (11)$$

Similarly, in a correlation experiment, determination of ρ_{00} requires observations from at least two θ angles. The angular distribution of the total intensity is given by

$$I(\theta,\phi) = (1-\rho_{00})\,\tfrac{1}{2}\,[1+\cos^2\theta-P_\xi\cos 2(\phi-\gamma)\cdot\sin^2\theta] + \rho_{00}\cdot\sin^2\theta \quad , \qquad (12)$$

replacing Eq. (4). Equation (12) may be written as

$$I(\theta,\phi) = B(\theta)[1-A(\theta)\cdot\cos 2(\phi-\gamma)] \quad , \qquad (13)$$

where

$$A(\theta) = \frac{(1-\rho_{00})\cdot P_\xi\cdot\sin^2\theta}{(1+\rho_{00})+(1-3\rho_{00})\cdot\cos^2\theta} \quad . \qquad (14)$$

The value of A in the scattering plane is

$$A(\tfrac{\pi}{2}) = \frac{1-\rho_{00}}{1+\rho_{00}}\cdot P_\xi < P_\xi \quad . \qquad (15)$$

i.e., a smaller amplitude than the amplitude P_ξ for the corresponding coherence analysis along z^n, see Eq. (9). Equation (14) also implies that

$$A(\tfrac{\pi}{4}) = P_\xi(1-\rho_{00})/(3-\rho_{00}) \quad . \qquad (16)$$

Defining the ratio $R = A(\pi/4)/A(\pi/2)$ one obtains

$$\rho_{00} = (3R-1)/(R+1) \quad . \qquad (17)$$

The general case is thus described by four parameters $(\gamma, L_\perp, P_\perp, \rho_{00})$ of which the three first can be determined from coherence analysis along $+z^n$. Notice that one may still have full coherence within the positive reflection symmetry, $P^+=1$.

The situation is summarized in Fig. 4, which shows the shapes of the charge clouds and below, in comparable scales, cuts along the principal axes in the atomic frame. In both cases (a) and (b) the alignment angle is 35° and the width parameter $P_\xi=0.6$, but the height parameter in (a) is $\rho_{00}=0$, i.e. positive reflection symmetry, while $\rho_{00}=1/3$ in (b). The angular momentum has no influence on the shape, and P_3 can be anywhere in the region $-0.8<P_3<0.8$, so that $P^+<1$. The parametrization suggested above is a natural development of

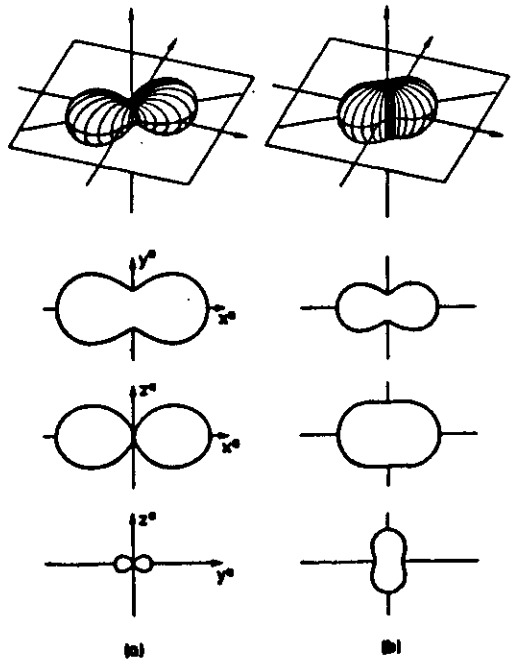

FIGURE 4

the semiclassical model put forward by Macek and Jaecks in Sec. III of their fundamental paper (12).

2.2.4. Relations to the Blum-Paixão parameters

Blum, Paixão and collaborators (13) were the first to realize and formulate a parametrization for the general case. Here we summarize their mathematics and give relations to the parameters defined above. Again the atomic basis of Fig. 1 is used, however this time quantized along $z^c = z^n$. The density matrix may be decomposed into two components with positive and negative reflection symmetry with respect to the scattering plane, expressible in terms of the Stokes parameters in the following way (tr ρ=1)

$$\begin{Bmatrix} \rho^c_{11} & \rho^c_{10} & \rho^c_{1-1} \\ \rho^c_{01} & \rho^c_{00} & \rho^c_{0-1} \\ \rho^c_{-11} & \rho^c_{-10} & \rho^c_{-1-1} \end{Bmatrix} = \begin{Bmatrix} \frac{1}{2}(\rho^c_{11}-\rho^c_{-11}) & \rho^c_{10} & -\frac{1}{2}(\rho^c_{11}-\rho^c_{-11}) \\ \rho^{c*}_{10} & 1-2\,\rho^c_{11} & -\rho^{c*}_{10} \\ -\frac{1}{2}(\rho^c_{11}-\rho^c_{-11}) & -\rho^c_{10} & \frac{1}{2}(\rho^c_{11}-\rho^c_{-11}) \end{Bmatrix}$$

$$+ (\rho^c_{11}+\rho^c_{-11})\,\frac{1}{2}\begin{pmatrix}1&0&1\\0&0&0\\1&0&1\end{pmatrix}$$

$$+ (1-(\rho^c_{11}-\rho^c_{-11}))\cdot\frac{1}{2}\begin{pmatrix}\frac{1}{2}(1-P_1) & \frac{1}{\sqrt{2}}(-P_2+iP_3) & -\frac{1}{2}(1-P_1)\\ \frac{1}{\sqrt{2}}(-P_2-iP_3) & 1+P_1 & \frac{1}{\sqrt{2}}(P_2+iP_3)\\ -\frac{1}{2}(1-P_1) & \frac{1}{\sqrt{2}}(P_2-iP_3) & \frac{1}{2}(1-P_1)\end{pmatrix}$$

$$+ (\rho^c_{11}+\rho^c_{-11})\,\frac{1}{2}\begin{pmatrix}1&0&1\\0&0&0\\1&0&1\end{pmatrix} \quad ,$$

where $\rho^c_{11} + \rho^c_{-11} = \rho^0_{00}$ is determined by P_1 and $P_{\parallel}$; cf. Eq. (10). Following Blum and Paixão we now define

$$\lambda \equiv \rho^c_{00}$$

$$\tilde{\chi} \equiv \arg(\rho^c_{10}) = -\arg(\rho^c_{01})$$

$$\cos\Delta \equiv |\rho^c_{10}|/(\rho^c_{00}\rho^c_{11})^{1/2} = |\rho^c_{01}|/(\rho^c_{00}\rho^c_{11})^{1/2}$$

$$\cos\varepsilon \equiv -\rho^c_{1-1}/\rho^c_{11} = -\rho^c_{-11}/\rho^c_{11}$$

so that

$$(1-\rho_{00})\cdot P_1 = \tfrac{1}{2}\,[\lambda(3+\cos\varepsilon) - (1+\cos\varepsilon)]$$

$$(1-\rho_{00})\cdot P_2 = -2(\lambda(1-\lambda))^{1/2}\cdot\cos\Delta\cdot\cos\tilde{\chi}$$

$$(1-\rho_{00})\cdot P_3 = 2(\lambda(1-\lambda))^{1/2}\cdot\cos\Delta\cdot\sin\tilde{\chi}$$

where $\rho_{00} = (1-\lambda)(1-\cos\varepsilon)/2$. Here $0\le\lambda\le1$, $0\le\tilde{\chi}\le2\pi$, $0\le\cos\Delta\le1$, $-1\le\cos\varepsilon\le1$. We may require $0\le\Delta\le\pi/2$ since $\operatorname{sgn}\Delta$ has no physical meaning. Similarly $0\le\varepsilon\le\pi$ since $\operatorname{sgn}\varepsilon$ has no meaning. If $\rho_{00}=0$ then $\varepsilon=0$.

2.3. Time evolution due to internal forces. Depolarization

2.3.1. The effect of fine structure

When the collision is over, the isolated atom develops under the influence of internal forces until the optical decay. Again, restricting ourselves to an excited P state, we shall first analyze the simplest case of electron spin S=1/2, and see how the shape and dynamics of the charge cloud changes in time, resulting in a modification of the observed radiation compared to the unperturbed case, S=0.

Consider first the shape: Referring to Fig. 4 it is most conveniently analyzed in terms of the molecular basis in the atomic frame for which the relevant density matrix elements at the time of excitation t=0 are given by

$$\rho^a_{xx}(0) = \tfrac{1}{2}(1+P_{\parallel}) \ , \quad \rho^a_{yy}(0) = \tfrac{1}{2}(1-P_{\parallel}) \ , \quad \rho^a_{zz}(0) = 0$$

which directly measure the relative length, width and height of the charge cloud. The shape now develops in time according to [see, e.g., Ref. (14)]

$$\rho^a_{xx}(t) = \rho^a_{xx}(0)\cdot G_2 + \tfrac{1}{3}(G_0-G_2)$$

$$\rho^a_{yy}(t) = \rho^a_{yy}(0)\cdot G_2 + \tfrac{1}{3}(G_0-G_2)$$

$$\rho^a_{zz}(t) = \quad 0 \quad \cdot G_2 + \tfrac{1}{3}(G_0-G_2)$$

where $G_0 = G_0(t) = 1$ and $G_2 = G_2(t) = 1/3\cdot[1+2\cos(\omega_{fs}t)]$; $\hbar\omega_{fs}$ is the energy splitting between the fine structure levels $^2P_{1/2}$ and $^2P_{3/2}$. Thus, as long as we assume $\rho_{ss}(0) = 0$, the height varies in time as

$$\rho_{00}(t) = \rho^a_{zz}(t) = \tfrac{2}{3}\,[1-\cos(\omega_{fs}t)] \qquad (18)$$

independent of $\rho^a_{xx}(0)$ and $\rho^a_{yy}(0)$. For the simple shape discussed previously in Fig. 2 and Fig. 4(a) having $P_{\parallel}=0.6$, Fig. 5(a) shows the (reversible) change in time of the shape, where the five situations correspond to $\omega_{fs}t=0$, $\pi/2$, π, $3\pi/2$, 2π, respectively, showing the quantum-beat phenomenon well known in e.g. beam-foil spectroscopy. Since the symmetry axes stay fixed in time the plot has been made for $\gamma=0°$.

Most collision experiments only monitor the time average of these beats, i.e. the limit $\tau_{fs} \ll \tau_{obs}$, though some intermediate situations, displaying various aspects of this beat phenomenon, have been reported (15,16). Averaging over time yields a charge cloud corresponding to $\omega_{fs}t = \pi/2$ or $3\pi/2$ (here we assume that $\tau_{fs} \ll \tau_{nat}$, so that the pattern has time to develop before decay); i.e.,

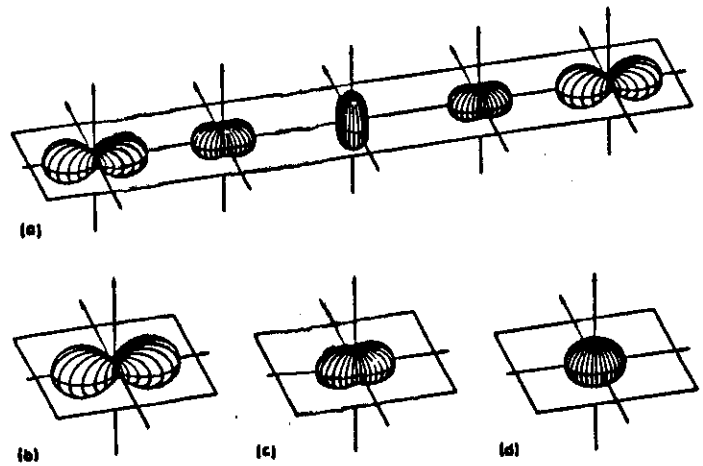

FIGURE 5

$$\langle \rho^a_{xx} \rangle_t = \frac{1}{3}\,\rho^a_{xx}(0) + \frac{2}{9} = \frac{7}{18}\,(1 + \frac{3}{7}\,P_\perp)$$

$$\langle \rho^a_{yy} \rangle_t = \frac{1}{3}\,\rho^a_{yy}(0) + \frac{2}{9} = \frac{7}{18}\,(1 - \frac{3}{7}\,P_\perp)$$

$$\langle \rho^a_{zz} \rangle_t = \qquad\quad \frac{2}{9} = \frac{2}{9} \quad .$$

thereby modifying the linear polarizations

$$P_{1,2}(S=1/2) = \frac{3}{7} \cdot P_{1,2}(S=0) \quad ,$$

provided that the sum of the two fine structure components, $^2P_{3/2} \rightarrow {}^2S_{1/2}$ and $^2P_{1/2} \rightarrow {}^2S_{1/2}$, is monitored.

The time evolution of the angular momentum $L_\perp(t)$ is best analyzed in the atomic basis, where the initial conditions are

$$\rho^a_{11}(0) = \frac{1}{2}\,(1+L_\perp)$$

$$\rho^a_{-1-1}(0) = \frac{1}{2}\,(1-L_\perp) \quad .$$

The time evolution is governed by (14)

$$\rho^a_{11}(t) = \frac{1}{2}\,L_\perp \cdot G_1 + \frac{1}{3}\,(G_0 + \frac{1}{2}\,G_2)$$

$$\rho^a_{-1-1}(t) = -\frac{1}{2}\,L_\perp \cdot G_1 + \frac{1}{3}\,(G_0 + \frac{1}{2}\,G_2)$$

with $G_1 = G_1(t) = 1/9 \cdot [7+2\cos(\omega_{fs}t)]$. Thus the spin-orbit coupling causes the angular momentum component along z^n to vary in time as

$$L_\perp(t) = \rho^a_{11} - \rho^a_{-1-1} = L_\perp \cdot \frac{1}{9}\,[7+2\cos(\omega_{fs}t)] \quad . \qquad (19)$$

The photon intensity $I_\perp(t)$ in the z direction varies in time as

$$I_\perp(t) = \rho^a_{11} + \rho^a_{-1-1} = \frac{1}{9}\,[7+2\cos(\omega_{fs}t)] \qquad (20)$$

in agreement with Eq. (18). Equations (19) and (20) show that $L_\perp(t)$ and $I_\perp(t)$ vary with the same amplitude, implying that $P_3 = (\rho_{-1-1}-\rho_{11})/(\rho_{-1-1}+\rho_{11}) = -L_\perp = -L_\perp^*$ stays constant in time and is thus not affected by the fine structure:

$$P_3(S=1/2) = P_3(S=0) \quad .$$

So, a measurement of the Stokes parameters for a $^2P \rightarrow {}^2S$ transition allows reconstruction of the shape and dynamics of the charge cloud created in the collision by multiplying the linear polarizations by a factor 7/3, while P_3 is unchanged. The average intensity $I_\perp = \langle I_\perp(t) \rangle = 7/9$ is reduced because of the change in photon angular distribution.

Table 1 summarizes the (average) intensity and the depolarization factors c_1 for circular and c_2 for linear polarization in the z^n direction for the cases S=1/2 and S=1, including also the individual fine structure components. General formulas may be found in (17).

2.3.2. The effect of hyperfine structure

In analogy to the fine structure effect, the presence of nuclear spin will cause further oscillatory behavior. We shall not present the details in general but refer to the literature (14) and here just give as an example the effect of further adding a nuclear spin I=3/2. The effect on the (time averaged) circular polarization is a reduction to almost half the size, while the linear polarization is reduced by almost a factor of eight, cf. Table 1.

TABLE 1

Transition		$I_\perp$	c_1	c_2
1 → 0:	$^1P \rightarrow {}^1S$	1	1	1
	$^2P \rightarrow {}^2S$	7/9	1	3/7
	$^2P_{1/2} \rightarrow {}^2S_{1/2}$	2/9	1	0
	$^2P_{3/2} \rightarrow {}^2S_{1/2}$	5/9	1	3/5
	$^3P \rightarrow {}^3S$	41/54	27/41	15/41
	$^3P_0 \rightarrow {}^3S_1$	2/27	0	0
	$^3P_1 \rightarrow {}^3S_1$	1/4	1/3	1/3
	$^3P_2 \rightarrow {}^3S_1$	47/108	45/47	21/47
1 → 3/2:	$^2P \rightarrow {}^2S$	209/300	325/627	27/209

Figure 5 illustrates the effect on the (time-averaged) shape by subsequently adding an electron spin S=1/2, (b) → (c), and a nuclear spin I=3/2, (c) → (d), leading to an almost isotropic charge distribution. This situation is close to the case of the $^7Li(2^2P)$ state, where, however, effects due to a finite lifetime, etc., also show up (16).

Fine and hyperfine structure may thus cause a severe reduction in measured anisotropy compared to the nascent charge cloud, provided of course that they have time to develop.

2.4. S→D excitation

S→D excitation has so far only been studied in a few cases. A D state has five substates of which, in the natural frame, the atomic basis states with M=2, 0, -2 have positive reflection symmetry with respect to the scattering plane, while M=1, -1 yield negative reflection symmetry. In the simple case where the excitation is fully coherent and the system possesses positive reflection symmetry, three amplitudes (a_2, a_0, a_{-2}) thus come into play. The normalization condition $|\vec{a}|=1$ and an arbitrary phase factor leave four real parameters to be determined. The dipole radiation pattern for a subsequent D→P decay is completely determined by the four parameters P_1, P_2, P_3, P_4 introduced above. One might think that a coherence analysis giving these four Stokes parameters determines the D state completely. However, this turns out not to be the case (18). Though characteristic parameters for the shape and dynamics of the charge cloud, like γ, $L_\perp$, $P_\perp$ and the relative height, still given by Eq. (10), can be evaluated, analysis shows that in general two D-states exist having identical dipole radiation patterns, one charge cloud being the mirror of the other one in the (x^a, z^a) plane. Here x^a is still the symmetry axis of the radiation pattern, but the charge cloud does not exhibit reflection symmetry with respect to this plane (18). Application of external fields, which break the symmetry even further and influence the time development of the charge cloud during the time from excitation to decay, is necessary in order to distinguish between the two possibilities (19).

3. ORIENTATION EFFECTS

We shall now address some central, not yet resolved problems of current interest, which may conveniently be discussed within the framework presented above. Our aim is to attempt to understand orientation effects, a feature unique for planar scattering experiments.

after Andersen et al. define $\hat{k}, \hat{k}'$ as the plane of scattering

$\hat{z}'$ as quantization axis, where $\hat{z}' = \frac{\hat{k} \times \hat{k}'}{|\hat{k} \times \hat{k}'|}$

$|\psi\rangle$ is the state function after scattering $s \to p$

then $|\psi\rangle = a_{+1}|1\rangle + a_0|0\rangle + a_{-1}|-1\rangle$

where $|1\rangle, |0\rangle, |-1\rangle$ are the three pure angular momentum states shown in the top three figures of Fig. 1 (Andersen p 3)
the state $|0\rangle$ can't be excited because it has negative reflection symmetry (mirror image scattering above and below the collision plane). Leave a_{+1}, a_{-1} to fully describe the collision, i.e., 3 parameters, just as before.

$$|\psi\rangle = a_{+1}|1\rangle + a_0|0\rangle + a_{-1}|-1\rangle = a_{+1}|1\rangle + a_{-1}|-1\rangle$$

the $|+1\rangle, |-1\rangle$ wavefunctions are:

$$|1\rangle = e^{i\varphi}\sin\theta \quad , \quad |-1\rangle = e^{-i\varphi}\sin\theta$$

where 

$$\therefore \langle\psi|\psi\rangle = |a_+|^2\sin^2\theta + |a_-|^2\sin^2\theta + a_+a_-^*e^{2i\varphi}\sin^2\theta + a_+^*a_-e^{-2i\varphi}\sin^2\theta$$

let $a_+ = a$ (real - set arbitrary phase to zero)

$a_- = be^{2i\delta}$: a, b, δ unknown.

IMPORTANT: conventionally $|a_+|^2 + |a_-|^2$ is normalized to unity. This means only 2 of 3 parameters can be determined: $|a_+|^2 + |a_-|^2 = 1$

or $a^2 + b^2 = 1$

$$\text{then } \langle\psi|\psi\rangle = \left\{1 + 2ab\left[\frac{e^{2i\delta - 2i\varphi} + e^{-2i\delta + 2i\varphi}}{2}\right]\right\}\sin^2\theta$$

$$= \{1 + 2ab\cos 2(\varphi - \delta)\}\sin^2\theta$$

this is an elliptical-like object with major axis at $\varphi = \delta$.
minor axis at $2(\varphi - \delta) = \pi$. Therefore positions of major & minor axes determine δ